CHAPTER 2

Carbon Nanotube-Based Inorganic Composites

Massimo Bottini, Marcia I. Dawson, Tomas Mustelin
Burnham Institute for Medical Research, La Jolla, CA 92037, USA

CONTENTS

1. INTRODUCTION

Nanotechnology is the science of manipulating and assembling matter at the atomic and molecular scale in order to fabricate novel materials with enhanced physical and chemical properties. Composites of nanoscale entities have potential for use in multifunctional systems, including optoelectronics, sensing, and catalysis.

Carbon nanotubes (NTs) are undergoing intense investigation to explore their unique morphological, electronic, mechanical, thermal, and optical properties [1]. In many cases, to fabricate nanodevices or composites capable of taking full advantage of their unique properties, NTs must be attached to other molecules, nanoparticles (NPs) or surfaces. In this chapter, we address the decoration of single-walled (SW) and multi-walled (MW) carbon NTs with metallic, semi-conducting, and insulating NPs. Various strategies have been developed involving both covalent or non-covalent functionalization of either pristine or acid-oxidized NT sidewalls with previously grown NPs and the in situ growth of NPs onto NTs.

The choice of a specific technique for NT decoration with NPs is usually dictated by the final application of the composite. Because NT-based electronic devices must retain the extraordinary electronic properties of NTs, in situ growth or noncovalent functionalization of pristine NTs is preferred. In the case of noncovalent functionalization, the forces between the NPs and the NT sidewalls would be too weak to guarantee mechanical stability. Techniques based on covalent functionalization could resolve this problem. However, because functionalization currently involves introducing carboxylic acid groups by oxidation in strong acids, the high aspect ratio of the NTs is destroyed and dramatic changes in their electronic properties occur. For each functional group introduced by oxidation, an equivalent number of π-electrons are removed from the conjugated π-system of the NT.

ISBN: 978-1-58883-131-0

Chemistry of Carbon Nanotubes
Edited by V. A. Basiuk and E. V. Basiuk
Volume 3: Pages (25–34)

NPs have been linked to NTs by linkers that can be a molecule, a macromolecule, or a polymer. The choice of the linker is dictated by the final application of the NT-NP nanoassembly. For example, for biosensorial applications NTs that are easily visualized by simple optical microscopy are useful. Therefore, the NPs should be fluorescent and the linker used to couple them to the NT sidewall should avoid the quenching of their fluorescence caused by interactions with the NTs, since the latter could provide an alternative, non-irradiative decay path for the photoexcited electrons of the NPs. On the other hand, for NT-based photoelectrochemical cell fabrication, the linker should permit electron transfer from the excited states of the NP (luminophore) into the conduction band of the NT (quencher).

2. METALLIC NANOPARTICLES

Various strategies have been developed to fabricate nanoassemblies of NTs and metallic NPs. Although we present the main techniques used to decorate NTs with gold nanoparticles (GNs) in this section, similar techniques have been used to link other metallic NPs to NTs. The decoration of pristine NTs (pNTs) and oxidized NTs (oxNTs) with previously grown NPs and the in situ growth of NPs onto NTs are described.

2.1. Pristine Carbon Nanotubes

2.1.1. Noncovalent Chemistry

pNT-GN nanoassemblies have been made using linkers that were hydrophobically anchored or adsorbed via π-π stacking interactions onto the sidewalls of pNTs.

Ellis et al. [2] reported the connection of octanethiol (OT)-capped GNs to pNTs by hydrophobic interactions [Figure 1]. Acetone molecules were first adsorbed onto the defects of pNT sidewalls through C—O—C interactions or resonance structures, so that their methyl groups extruded from the pNT surface. OT-capped GNs were then anchored onto pNTs through hydrophobic interdigitation between the acetone methyl groups and the octyl chains of the self-assembled molecular (SAM) layers capping the GNs. Interdigitation between adjacent GNs adsorbed onto the pNTs

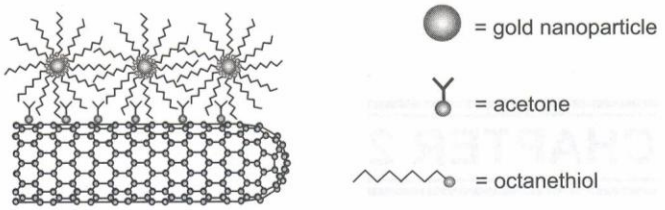

Figure 1. Decoration of pristine carbon nanotubes with octanethiol-capped gold nanoparticles using acetone as linker [2].

avoids their coalescence, resulting in wire-like structures consisting of large polycrystals [3], and permits modulation of the distance between GNs by adjusting SAM chain length and structure. The latter property could be useful for modulating quantum effects (e.g., single-electron hopping and coulomb blockade) to enable the molecular-level design of nanodevices for switching, sensing, and information storage.

Polycyclic aromatic molecules have been observed to adsorb onto pNT sidewalls through π-π stacking interactions. Their adsorption has been exploited as a method to decorate pNTs with macromolecules, silica NPs, and organometallic molecules. Mono- and polycyclic aromatic-ring terminated alkylamines [2-phenylethylamine, *N*-(1-naphthyl) ethylenediamine and 1-pyrenemethylamine] have been used by Ou et al. [4] as linkers for fabricating NT-GN nanoassemblies. The surface of GNs was modified by the alkylamines through interaction of the lone electron pair of their nitrogen atom. The modified GNs were subsequently adsorbed onto pNT sidewalls via π-π stacking interactions between the aromatic rings of the linker and the pNTs [Figure 2 (A–C)]. The linkage bond of the NT-GN nanoassembly was monitored by the authors by UV-Vis absorption and photoluminescence spectroscopies. The absorption vibronic features of the aromatic rings were perturbed upon complexation of the linker to the GNs, indicating strong interactions between the π-electron clouds of the aromatic rings and the plasmon electrons of the GNs. The absorption vibronic features of the aromatic rings were further perturbed upon the adsorption of the modified GNs onto pNT sidewalls. The surface plasmon resonance (SPR) absorption band of the GNs was also perturbed upon complexation,

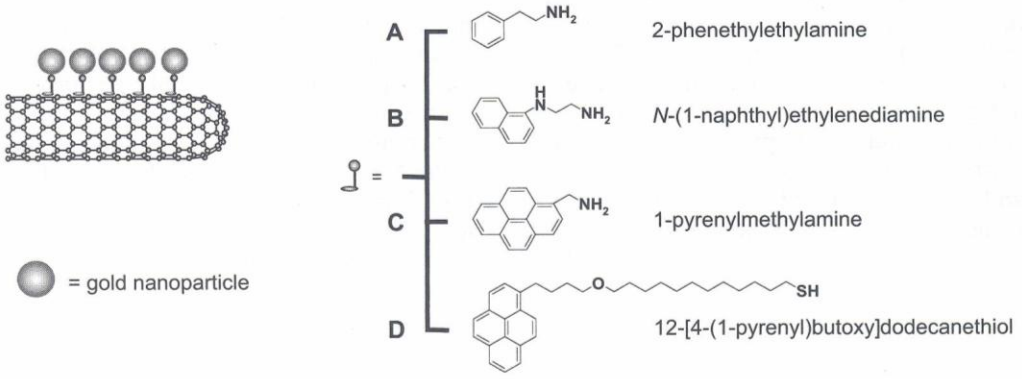

Figure 2. Decoration of pristine carbon nanotubes with gold nanoparticles using polycyclic aromatic ring-terminated alkylamines linkers [4, 6].

indicating interparticle plasmon coupling of the GNs that were in close contact with one another. Generally speaking, the absorbance spectrum is able to give information about a system composed of colloidal GNs. According to Zhong et al. [5], the position of the SPR absorption band depends on particle size, the interparticle distance, and the interaction of GNs with other molecules in the colloidal dispersion. Thus, a red shift of the SPR band is attributed to interparticle plasmon coupling, a phenomenon observed even when just a few GNs are clustered. This red shift in the plasmon of GNs deposited onto pNTs suggests that the GNs were densely packed onto the surface of the tubes. Finally, quenching of the photoluminescence of the aromatic rings upon complexation of the GNs and pNTs indicates electron transfer (ET) between the aromatic rings (donor) and the two components (pNT and GN) of the nanoassembly, which function as quenchers.

Spectroscopic analyses were also used by Liu et al. [6] to study the decoration of pNTs with GNs to which 12-[4-(1-pyrenyl) butoxy] dodecanethiol (PBT) had been linked through thiol group-GN interaction. The pyrenyl groups then were adsorbed onto the pNT surfaces [Figure 2 (D)]. The fluorescence of PBT was quenched moderately by its binding to the pNTs and almost totally quenched through the further binding of GNs, suggesting ET from the linker and the pNTs as well as the GNs. Moreover, the authors observed an enhanced Raman response. The two main contributions to the surface increase of Raman scattering of NTs on metallic surfaces occur through 'electromagnetic' and 'chemical' mechanisms [7]. The former is caused by an increase in the electromagnetic field at or near the metallic surface, and the latter is caused by ET between the metallic surface and the NTs and strongly depends on the NT electronic structure. Therefore, the observed increase in the Raman response suggested ET between the GNs and the pNTs through the linker.

2.1.2. Covalent Chemistry

The noncovalent decoration of pNTs with GNs was described above in Section 2.1.1. pNTs have also been covalently functionalized using cycloaddition reaction. Coleman et al. [8] reported the cyclopropanation of SWNTs under Bingel reaction conditions with GNs used as "chemical tags" to confirm the presence of reacted surface sites [Figure 3]. SWNTs were allowed to react with the carbine generated from treatment of diethyl 2-bromomalonate with the base (1,8-diazabicyclo[5.4.0]undecene, DBU), transesterified by stirring with an excess of 2-methylthioethanol to introduce a thioether linker, then exposed to gold colloids to "tag" the cyclopropane groups to verify that the pNTs were cyclopropanated. They obtained uniformly GN-decorated pNTs.

2.2. Oxidized Carbon Nanotubes

2.2.1. Electrostatic Interactions

Jiang et al. [9] reported that GNs could be noncovalently attached to oxidized MWNTs using a polyelectrolyte as an electrostatic bridge [Figure 4]. First, MWNTs were oxidized by suspending in a concentrated sulfuric acid/nitric acid mixture (3:1 v/v) and sonicating. FT-IR analysis indicated that the acidic oxidation introduced four functional groups onto the NTs, namely hydroxyl, carboxyl, carbonyl, and sulfonyl groups. The oxNTs were coated with a cationic polyelectrolyte [poly (diallyldimethylammoniumchloride), PDAC] that adsorbed onto the NT surface because of the electrostatic interactions between the negative carboxate groups and the polyelectrolyte. Finally, negatively-charged GNs were anchored onto NTs through electrostatic interaction between the polyelectrolyte and the GNs. The resulting NT-GN structure showed quite uniform decoration of the GNs on the NT walls and ends in correspondence to the location of the functional groups. Therefore, the reported technique could represent an excellent method for monitoring the presence of charged functional groups on the surface of NTs.

Kim et al. [10] reported a similar procedure to decorate oxNTs with GNs. MWNTs were chemically functionalized by oxidation using ultrasonication in a sulfuric acid/nitric acid mixture (3:1 v/v) for 1 to 8 h. The authors showed that only NTs treated longer than 4 h were colloidally stable in aqueous media for at least 24 h. Positively-charged GNs were electrostatically deposited onto oxNTs that were negatively charged by deprotonation of their carboxylic acid groups introduced during chemical oxidation [Figure 5(a)]. In addition, positively-charged GNs were anchored onto negatively-charged NTs fabricated by the deposition of the positively-charged polyelectrolyte PDAC, followed by

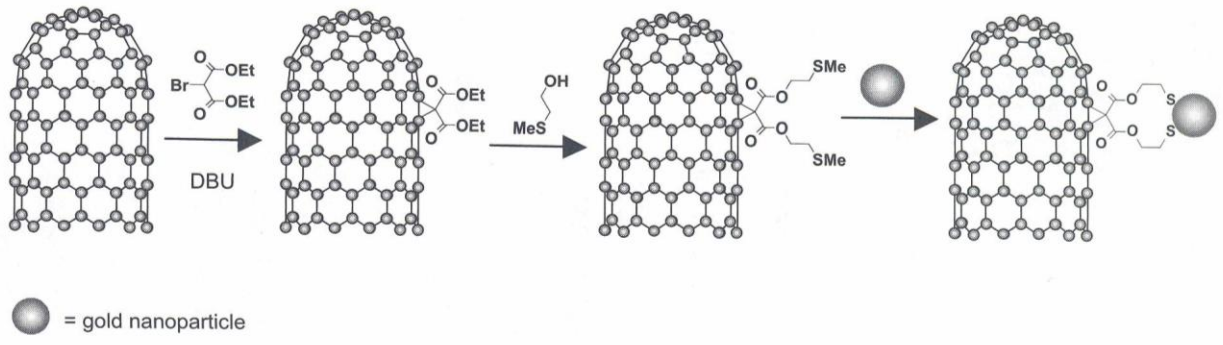

Figure 3. Decoration of pristine carbon nanotubes with gold nanoparticles by cyclopropanation of NTs using diethyl 2-bromomalonate under Bingel reaction conditions, followed by their transesterification with 2-methylthioethanol [8]. DBU = 1,8-diazabicyclo[5.4.0]undecene.

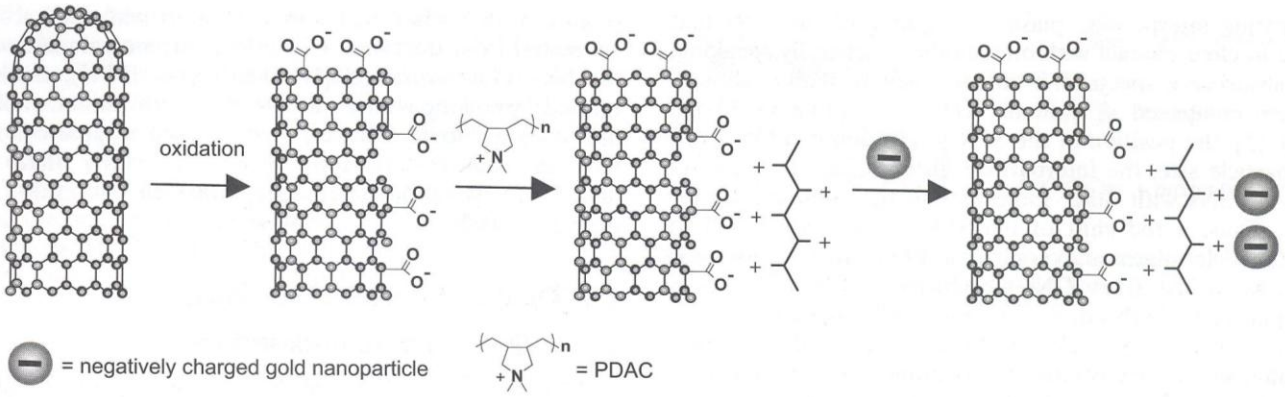

Figure 4. Decoration of oxidized carbon nanotubes with gold nanoparticles using a cationic polyelectrolyte [poly(diallyldimethylammonium-chloride), PDAC] as linker [9].

a negatively charged polyelectrolyte [poly (sodium 4-styrene-sulfonate), PSS] onto oxNTs [Figure 5(b)]. In the latter case the density of the linked GNs was higher than that achieved by those directly anchoring onto oxNT. The authors rationalized that the higher loading was caused by the polyelectrolyte coating increasing the number of reactive sites.

2.2.2. Covalent Chemistry

Liu et al. [11] first reported the oxidative shortening of NTs by refluxing them in strong acid followed by the covalent derivatization of the resultant open ends with GNs. The carboxylic groups, which are introduced by oxidation, mainly occurred at the NT ends. These groups were converted to the corresponding acid chlorides by reaction with $SOCl_2$. Subsequent treatment with $NH_2{-}(CH_2)_{11}{-}SH$ in toluene produced NTs linked to the alkanethiols through amide bonds. Finally, GNs were linked to the thiol groups to form NT-GN nanoassemblies constituted of short oxNTs having GNs mainly at their ends [Figure 6].

Similarly, Hu et al. [12] reported the functionalization of oxNTs with thiol groups through a molecule containing thiol groups and halogen. The loading of the GNs onto NT sidewalls was checked by absorbance and energy dispersive X-ray spectroscopies and by transmission electron microscope (TEM). The latter showed that the GNs were concentrated in the sidewall sites of higher curvature. This result is consistent with the view that the sidewall sites of higher curvature are more defective, are oxidized first, and present higher concentration of carboxylic acid groups after the acid treatment.

2.3. In Situ Growth

In the previous paragraphs we described decorating NTs with previously grown NPs. On the other hand, many researchers have reported the in situ growth of metallic NPs onto NTs by such methods as electrochemical deposition, electroless deposition without reducing agents, and substrate-enhanced electroless deposition.

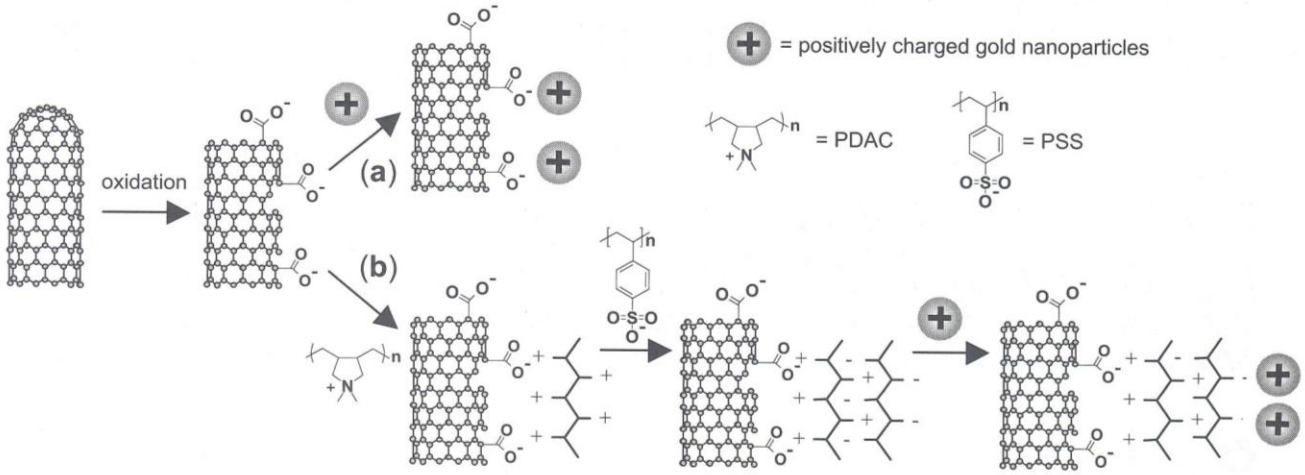

Figure 5. Decoration of oxidized carbon nanotubes with gold nanoparticles by direct deposition (a) or by using a bilayer of cationic [poly(diallyldi-methylammoniumchloride), PDAC] and anionic [poly(sodium 4-styrenesulfonate), PSS] polyelectrolytes as the linkers (b) [10].

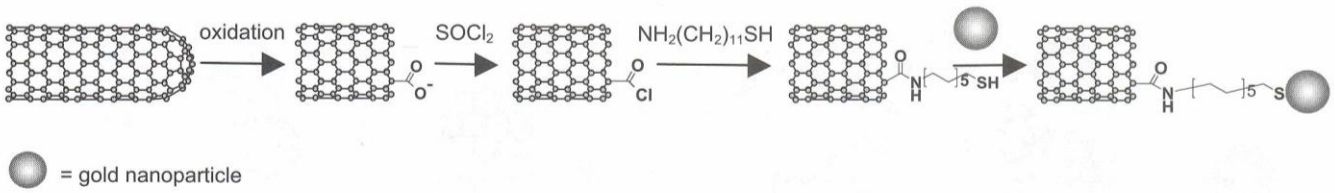

Figure 6. Functionalization of oxidized carbon nanotubes by a two-step reaction: the carboxylic groups introduced by the acid-treatment are activated as acyl chloride groups, which react with amino-terminated alkanethiols to form amide bonds through a nucleophilic acyl substitution [11]. The exposed thiol groups were then linked to gold nanoparticles.

Quinn et al. [13] reported the electrodeposition of noble metals (Au, Pt, Pd) under direct potential control onto the sidewalls of SWNTs that act as a nonsacrifical template for the grown clusters [Figure 7]. The authors found that the size of the metal clusters increased significantly as the potential was made more negative and that, for a given nucleation potential, the size of the clusters increased with both deposition time and metal salt concentration.

Choi et al. [14] reported the spontaneous formation of Au and Pt NPs on the sidewalls of SWNTs when the latter are immersed in corresponding metal salt solutions. The reported process differed from traditional electroless deposition in that no reducing agents or catalysts were required. The highly selective metallic NP deposition onto the SWNTs resulted from direct redox reaction between metal ions and NTs. Electron transfer from NTs to metal ions was probed electrically, as the hole injection into SWNTs causes an increase in the electrical conductance. The direct electron transfer between NT and metal ions depended on their relative redox potential. The Fermi level of NT is about +0.5 V above the redox potential of the standard hydrogen electrode (SHE) and, therefore, well above those of $AuCl_4^-$ (+1.002 V) and $PtCl_4^{2-}$ (+0.775 V), explaining the spontaneous electron transfer from NTs to the metallic anions. While this technique is an extremely simple and elegant method to decorate NTs with Au and Pt NPs, it fails for the reductive deposition of metal ions such as Cu^{2+}, Ag^+, and Ni^{2+} because their redox potentials are lower than that of the NTs. This problem was resolved by Qu et al. [15] using a Substrate-Enhanced Electroless Deposition (SEED) technique. They were able to reduce metal ions with a redox potential lower than that of the NTs to metallic NPs onto NTs by supporting the NTs on a metal substrate having a redox potential below that of the metal ions to be reduced into NPs [Figure 8]. The deposition of metallic NPs was achieved via the redox reaction of a galvanic cell, in which the NT acted as a cathode for metal deposition from the reduction of metal ions in solution, while the metal substrate served as an anode on which the metal atoms are oxidized and retained on the substrate. As demonstrated by the authors, this technique permitted the deposition of any metallic NP on a conducting NT as long as the redox potential of the substrate metal (Sub^{n+}/Sub^0) was lower than that of the metal ions (M^{z+}/M^0) in solution.

3. SEMI-CONDUCTING NANOPARTICLES

A novel strategy for altering the electronic properties of NTs is to chemically functionalize them with groups or structures, the intrinsic properties of which are electronically configurable. One such structural family is composed of semi-conducting nanocrystals CdSe, CdS, ZnO, and ZnS, which are also known as quantum dots (QDs). These materials exhibit strong size-dependent optical and electrical properties [16, 17]. Their high luminescence yields and potential of adjusting their emission and absorption wavelengths by selecting for nanocrystal size make QDs attractive for constructing optoelectronic devices with tailored properties [18, 19] or for in vivo biosensing applications [20].

3.1. Oxidized Carbon Nanotubes

Several groups have reported the decoration of oxNTs with CdSe semiconductor nanocrystals using organic molecule

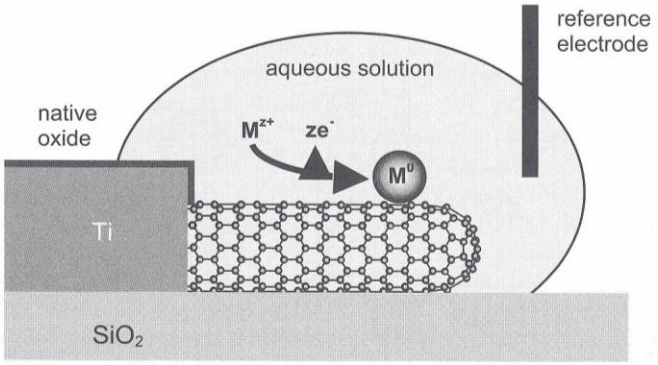

Figure 7. Electrodeposition of noble metals under direct potential control onto sidewalls of single-walled carbon nanotubes [13].

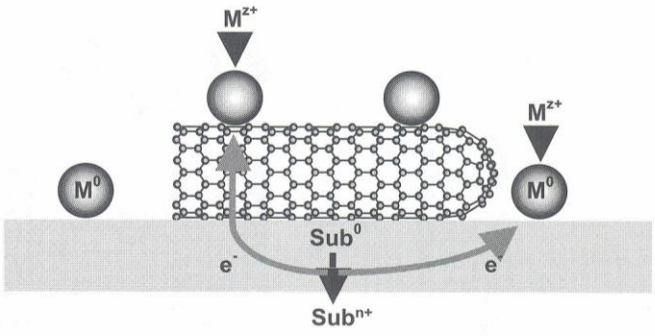

Figure 8. Electrodeposition of metal nanoparticles onto single-walled sidewalls through Substrate-Enhanced Electroless Deposition (SEED) [15].

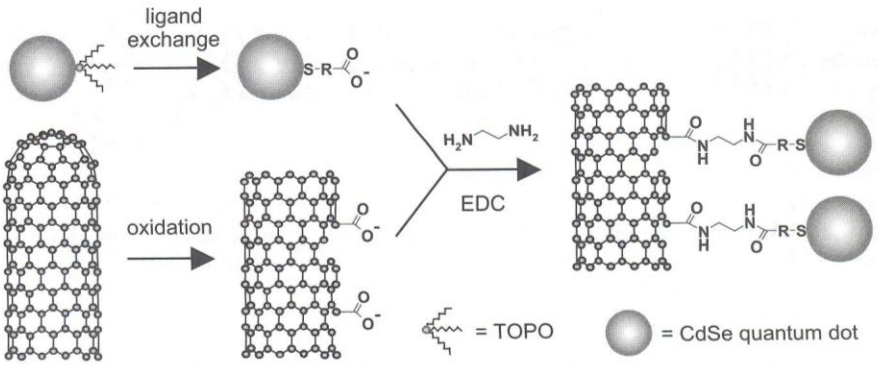

Figure 9. Functionalization of oxidized carbon nanotubes with carboxylated quantum dots using a diamine linker [18]. TOPO = trioctylphospine oxide.

linkers. In a report, CdSe QDs capped with trioctylphospine oxide (TOPO) were synthesized from purified dimethylcadmium as a precursor [18]. Subsequently a ω-carboxy alkyl thiol replaced the TOPO capping to give carboxylic acid-terminated CdSe QDs, which were then linked to oxNTs through diamide bonds between the diamine linker (ethylenediamine) and the carboxyl groups on the oxNTs and substituted QDs [Figure 9]. The authors observed the disappearance of the lowest energy exciton in the NT-QD nanoassembly corresponding to the band-gap excitation in the original semiconductor QD. This result suggested that energy transfer (ET) occurred from the donor (QD) to the acceptor (oxNT).

Haremza et al. [19] achieved a NT-QD nanoassembly following a similar procedure [Figure 10]. QDs were synthesized using variations of the methods developed by Murray et al. [21] and Qu et al. [22]. A ZnS coating over the CdSe QD core improved the quantum yield by passivating carrier trap sites (surface dangling bonds) and decreased the toxic nature of the core. The TOPO on the surface of ZnS-encapsulated CdSe QD was displaced for the amino-terminated aliphatic thiol, 2-aminoethanethiol, through which the QDs were linked to oxNTs functionalized as aryl chloride by treatment with thionyl chloride. In contrast to the results of Banerjee et al. no evidence of any electronic state coupling or large ET between the QDs and the oxNTs was observed. This result was rationalized on the basis that any electronic state coupling between the two materials would imply significant overlapping between their electronic wave functions. However, because the electron and hole wave functions would be well confined in a CdSe QD, no significant coupling to external electronic states would be expected. Moreover, the absence of ET may be caused by differences in the NT preparation method or in the specific linker between the oxNTs and QDs. The reported technique represents an improvement compared to those previously described because it circumvents the undesirable cross reactions that yields large clusters of NTs and QDs, which are not suitable for practical nanoelectronic applications. The morphology of NT-QD nanoassembly observed by these authors appeared to depend on NT length. When relatively long oxNTs (>200 nm) were used, the QDs decorated the NT sidewalls, whereas use of short oxNTs (<200 nm) led to QDs attached primarily the NT ends. These results were thought to occur because the shorter oxNTs have carboxylic groups mainly on their tips and have far fewer sidewall defects than long oxNTs. Therefore, selective decoration of NTs would be possible if the oxidation process were controlled. Ravidran et al. [23] reported an elegant procedure for the exclusive attachment of ZnS-encapsulated CdSe QDs onto NT ends [Figure 11] by using MWNTs. Selective carboxylation on MWNT termini has another advantage. As indicated by Haremza et al. sidewall functionalization disrupts the π-bonding symmetry of the

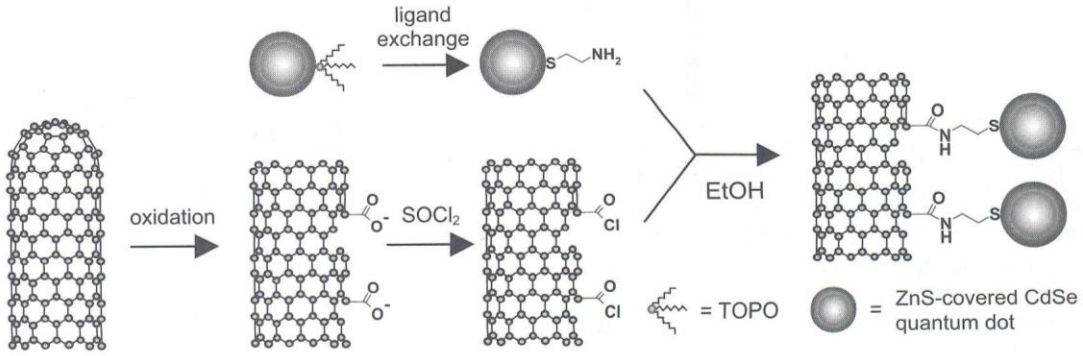

Figure 10. Functionalization of oxidized carbon nanotubes by a two-step reaction: the carboxylic groups introduced by the acidic oxidation-treatment are activated to acyl chloride that reacts with amino-terminated quantum dots to form amide bonds [19]. TOPO = trioctylphospine oxide.

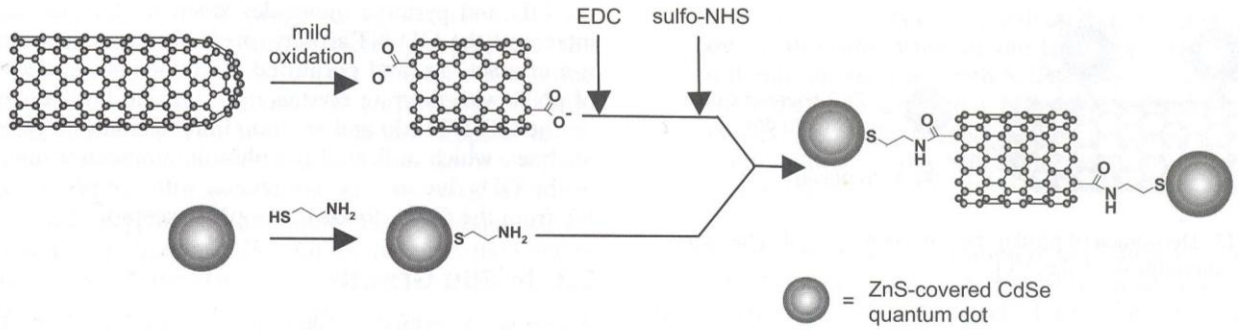

Figure 11. Decoration of the tips of oxidized carbon nanotubes with ZnS-encapsulated CdSe quantum dots through an amide bond [23]. EDC = 1-Ethyl-3-[3-dimethylaminopropyl]carbodiimide hydrochloride; sulfo-NHS = *N*-hydroxysulfosuccinimide.

sp^2-hybridization of the NTs to compromise their unique electronic properties necessary for electronic devices, whereas sidewall oxidation is acceptable for applications such as biosensing and for the realization of composites. Because electron transport in MWNTs is confined to the outermost shell while intershell interactions are weak, MWNTs preferentially oxidated at the tips allowed the authors to construct a NT-QD nanoassembly for electronic applications. Their strategy employed only mild oxidation conditions, namely a brief reflux in nitric acid to introduce terminal carboxylic acid groups, and was based on the assumption that fewer sidewall defects would be present in MWNTs due to the larger radius of curvature of MWNT.

3.2. Pristine Carbon Nanotubes

The previous techniques of decorating NTs with semiconducting QDs employed oxNTs and led to nonuniform surface coverage as the NPs were linked to the oxNTs at their open ends and sidewall defects where carboxylic groups introduced by oxidation are localized. A high degree of NT functionalization can appreciably alter band gaps and long-range conjugation. While for biosensorial applications electronic properties are not fundamental, for donor-acceptor systems intact electronic properties are extremely important. Thus, the linkage chemistries must control contact between electron donors and electron acceptors and preserve NT electronic structure. Successful examples are polymer wrapping, macromolecular adsorption, and π-π interactions with aromatic molecules.

Olek et al. [24] reported a novel strategy for the fabricating of NT-QD nanoassemblies. pNTs were prefunctionalized by nondestructively wrapping with a polymer so that no defects were introduced onto the NT sidewalls. QDs were covalently linked to the amine groups extruding from the polymer surface by ligand exchange chemistry. By choosing the kind of polymer the authors were able to control the contacts between electron donors (QDs) and electron acceptors (pNTs), thereby allowing or preventing the quenching of fluorescence due to charge transfer or tunneling from photoexcited QDs to pNTs. In particular, poly (allylamine hydrochloride)-coated pNTs quenched the fluorescence of their linked QDs, while pNTs coated by a thick and uniform layer of SiO_2 did not exhibit fluorescence quenching. The authors postulated that the large band gap and thickness of the silica layer would prevent quenching by both charge transfer and electron tunneling.

The prevention of the fluorescence quenching of QDs on pNTs by the polymeric linker would permit visualization of pNTs by routine fluorescent microscopy and their use as photoluminescent probes. Sodium dodecyl sulfonate (SDS) was reported to disperse pNTs in an aqueous environment through interaction of its hydrophobic dodecyl tail with the carbonaceous NT sidewall and expose the hydrophilic sulfonate head to the environment [25]. Chaudhary et al. [26] reported that small bundles of SDS-wrapped pNTs could be visualized by decorating them with ZnS-covered CdSe QDs, in which the Zn^{2+} ions were coordinated with the sulfonate oxygens on the NT surface [Figure 12]. The nanoassembly was visualized by routine fluorescence microscopy because the SDS layer prevented fluorescence quenching due to charge injection from the excited states of the QDs into the conduction band of the pNTs, which functioned as quenchers.

Functionalization of both SWNTs and MWNTs with macromolecules has gained increasing interest because of their use in constructing supramolecular nanoassemblies for biosensors and intracellular protein transporters. Streptavidin (Str), which is a 64-kDa tetrameric protein having a 5-nm diameter, has applications in anticancer therapies and diagnostics. Str adsorbs onto the sidewalls of pristine MWNTs [27, 28] and oxidized SWNTs [29]. Our research group decorated pNTs with Str-conjugated ZnS-encased CdSe QDs [Figure 13] [30]. The resulting NT-Str-QD nanoassembly fully dispersed in physiologic buffer and was visible

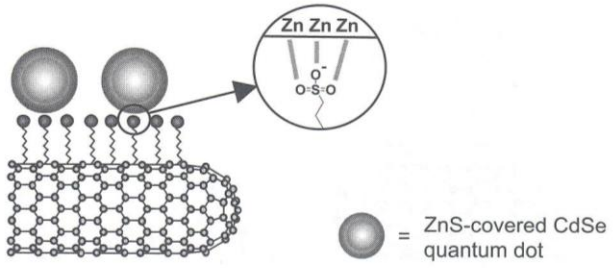

Figure 12. Decoration of pristine carbon nanotubes with ZnS-encapsulated CdSe quantum dots through the coordinative affinity of zinc ions to oxygen atoms in the sulfonate groups of the surfactant wrapping the nanotubes [26].

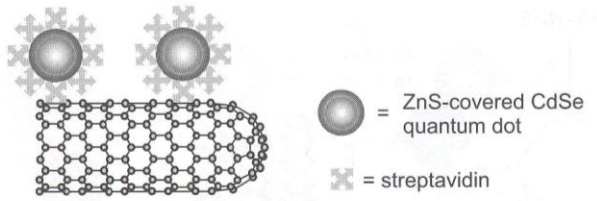

Figure 13. Decoration of pristine carbon nanotubes with quantum dots using streptavidin as a linker [30].

by conventional fluorescent microscopy. The latter property suggests that using Str as a macromolecular linker avoids ET from semiconducting QDs to the pNT. We investigated the ability of the NT-Str-QD nanoassembly to function as a multivalent intracellular fluorescent nanoprobe in Jurkat T leukemia cells. The nanoassembly was internalized by Jurkat T cells through receptor-mediated endocytosis and then partially released to lysosomes. Therefore, the NT-Str-QD represents a potentially excellent scaffold for constructing intracellular multivalent nanoprobes.

While using particular polymers to link pNTs and QDs would avoid QD-NT ET and permit the use of fluorescent NTs for sensorial applications, use of aromatic molecules as linkers would facilitate ET to permit photoactive material applications. Guldi et al. [31] nondestructively decorated pNT sidewalls with 1-(trimethylammoniumacetyl) pyrene (pyrene$^+$) that adsorbed through π-π interactions. The positively-charged trimethylammonium group allowed the pNTs to associate with negatively-charged, thioglycolate-stabilized, size-quantized CdTe QDs to produce a photoactive supramolecular nanostructure [Figure 14]. The strong electronic interactions in the ground and excited states of this nanoassembly were responsible for the favorable charge-transfer between its components. This result allowed Guldi et al. [31] to prepare a novel hybrid cell by sequential layering that, in response to visible light irradiation, performed as a photoelectrochemical device.

A similar noncovalent method for making CdSe-decorated pNTs that was based on the π-π interactions between pNTs and aromatic molecules was reported by Li et al. [32]. The TOPO on the QDs was displaced by pyridine molecules. Because CdSe QDs display good electron affinity and pyridine is a good electron donor, due to the isolated electron pairs on nitrogen, coordination between

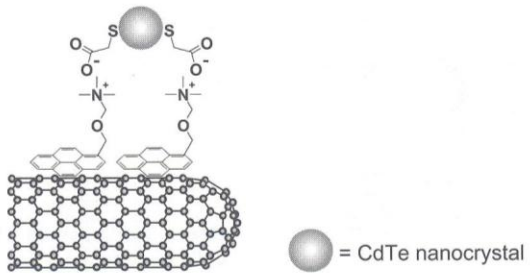

Figure 14. Decoration of pristine carbon nanotubes using a bifunctional linker [1-(trimethylammoniumacetyl)pyrene] adsorbed onto nanotubes sidewalls through via π-π interactions and electrostatically linked to thioglycolic acid-stabilized quantum dots [31].

the QD and pyridine molecules is stable. Ligand exchange increased the QD-NT affinity, probably through conjugated π-π interactions, and permitted the nonchemical decoration of pNTs with discrete crystals or a uniform layer depending on the QD/NT ratio and reaction time. Raman spectroscopic analyses, which indicated the photoluminescence quenching of the QDs due to their interaction with the pNTs, suggests ET from the CdSe donor to the pNT acceptor.

3.3. In Situ Growth

Above we described covalent and noncovalent decoration of NTs with chalcogenide NPs using linkers either attached at the ends and sidewalls defects of oxNTs, or hydrophobically adsorbed onto the sidewalls of pNTs, respectively. Their construction generally required multiple steps with variable yields and necessitated intermediary linkers. Both pristine and oxidized NTs have also been used as templates for direct thermal growth of CdSe [33, 34], ZnO [35], and ZnS [36] QDs or in situ wet chemical synthesis of CdS [37–39], ZnS [40], SnO_2 [41], and TiO_2 [42] QDs. Independent from these reported techniques it was observed that introducing functional groups on the NT surface benefited QD growth. For examples, Banerjee et al. reported the in situ thermal growth of CdSe and CdTe QDs onto the sidewalls of heavily oxidized SWNTs [33] and MWNTs [34]. This technique involved metal cation coordination to oxygenated, surface functional groups on the NTs, which then acted as specific nucleation sites for the growth of NT-QD interconnects. Oxidation opened and derivatized most of the NT ends as well as attacked occasional sidewall defect sites. The generated functional groups were expected to be carboxylic acids, alcohols, and ketones. These functionalized, oxygenated NTs were used as templates and ligands to grow QDs. The degree of QD immobilization scaled with the extent of NT oxidation. Only an aggressive oxidation regime enabled a high surface coverage by QDs on the open ends and serrated edges of the NTs. Few, if any, QDs were observed coordinated with pristine or weakly oxidized NTs. Crystal growth was predominantly wurtzite in structure, though at least some crystals appeared to have cubic morphology of zinc blend. The in situ-generated QDs varied widely in their shape and size. The anisotropic QD formation could be caused by the NT bulk, which would spatially hinder access to one side of the growing crystallite, thereby causing variations in crystal lattice. The degree of NT on the shape and dimension of the QD depended on such factors as functional group density at particular sites, site geometry, and functional group separation on the same or adjacent tube.

4. INSULATING NANOPARTICLES

Silica nanoparticles (SNPs) have been widely used for biosensing and catalytic applications due to their large surface area-to-volume ratio, straightforward manufacture, and the compatibility of silica chemistry to covalent coupling of biomolecules. The physical (diameter and porosity) and chemical properties of SNPs doped with fluorescent, magnetic, or biological macromolecules can be easily tuned. Therefore, carbon NT-SNP could be an excellent scaffold on which to construct higher-order assemblies.

Polymeric NPs can be prepared by several methods, including the widely used Stobër technique [43] and the water-in-oil nanoemulsion system [44]. The former is based on hydrolysis of a silica precursor in an alcoholic medium containing ammonia. The latter uses water droplets inside of reverse micelles as nanoreactors so that the size of the final NPs is regulated mainly by the dimension of the water droplets and, therefore, by the molar ratio of water to surfactant (w) and precursor (h). Other relevant parameters are molar ratio of precursor to catalyst (n), precursor reactivity, and reaction time (t) and temperature (T).

Our research group explored several techniques to fabricate nanoassemblies between SNPs and NTs [Figure 15] [45–47]. As illustrated in Figure 15, silylation both of pristine and oxidized NTs employed a silica precursor adsorbed onto pNTs through a pyrenyl group and coupled to oxNTs through a carboxamide bond, respectively. SNPs were also prepared separately and then coupled to NTs (method I) or grown directly on NTs in a water-in-oil nanoemulsion (method II).

The resulting nanoassemblies were characterized by the following properties:

1. SNP loading depended on silylation level of NT sidewalls.
2. SNP decoration occurred only at NT sites functionalized with silane, whereas the bare graphitic NT sidewall did not associate with SNPs.
3. Both methods decorated NTs with individual SNPs. However only the second method achieved a uniform silica coating on the NTs under particular conditions of synthesis.

Non-destructive functionalization of pNT sidewalls was conducted by the adsorption of a pyrenyl-terminated silica precursor onto the pNTs. The level of silylation of pNTs was tuned by the weight ratio between the silica precursor (tetramethylorthosilicate or tetraethylorthosilicate) and the NTs. Silylation of oxNTs was conducted by coupling an amino-terminated silica precursor (aminopropyltrimethoxysilane or aminopropyltriethoxysilane) to the carboxylic groups of oxNTs. The level of silylation of oxNTs depended on their oxidation level. By mild oxidation it was possible to introduce carboxylic groups only at the NT tips so that nanoassemblies were composed of short NTs having SNPs only at their ends. This result was not achieved by simple adsorption onto pNTs, which could not be spatially controlled.

In method I, previously grown SNPs were linked to silylated NTs. The morphology of the resulting nanoassemblies

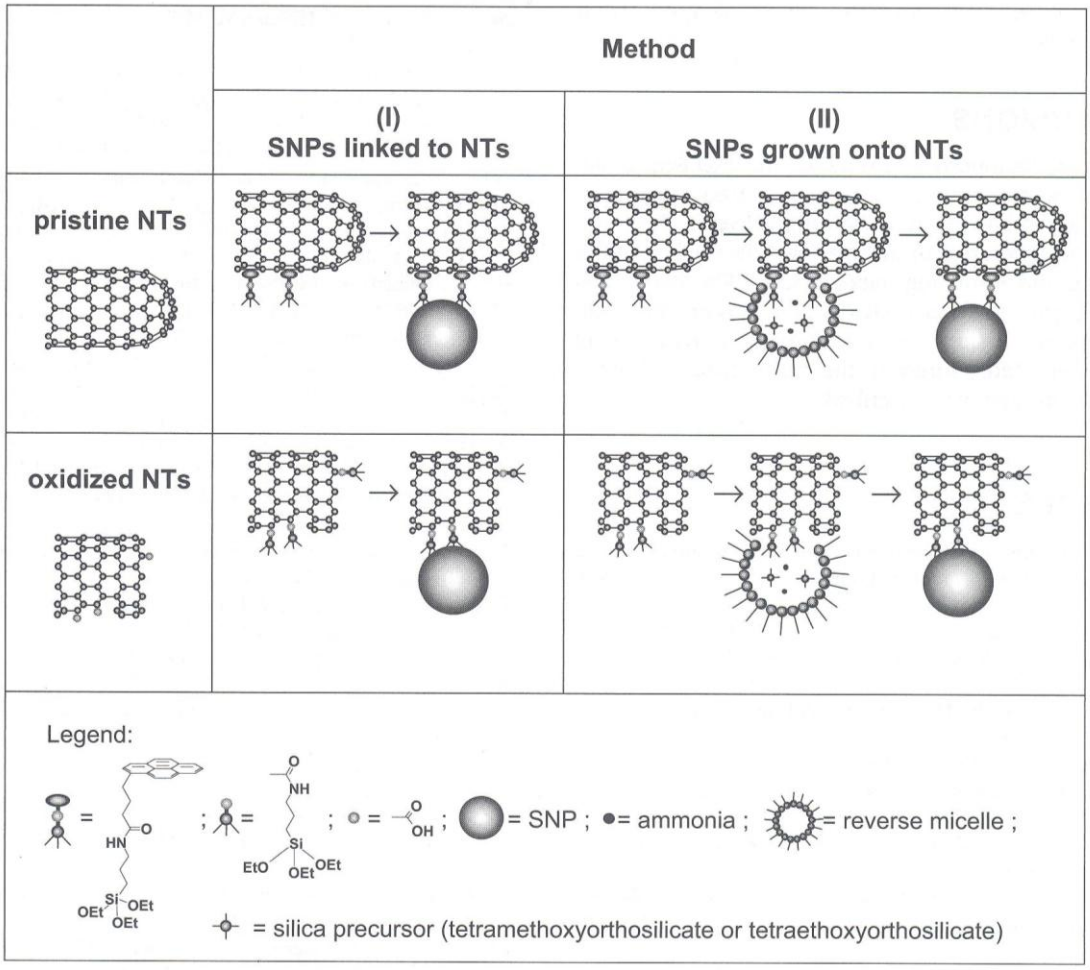

Figure 15. Functionalization of both pristine and oxidized carbon nanotubes (NT) with silica nanoparticles (SNP) [43–45].

was composed of full-length or shortened NTs decorated with SNPs. In method II, the SNPs were grown directly on the silane groups extruding from the NT sidewalls using a water-in-oil nanoemulsion system. SNPs that had a diameter smaller than that of the NTs grew individually on the NT sidewalls, whereas larger diameter SNPs formed a uniform coating around the NT if its level of silylation was high. Small reverse micelles, having approximately the same diameter as the NTs, were not able to totally embed the NTs and, therefore, could only nucleate the growth of the SNPs on the NT surface. Large reverse micelles were able to fully embed the NTs to nucleate growth of the SNPs around the NTs. If the level of silylation was high, the micelles were close enough to fuse and totally embed the NTs to allow the growth of a uniform layer of silica around the NTs.

Our research group fabricated the nanoassemblies composed of full-length and oxidized NTs and SNPs doped with a ruthenium complex fluorophore using method I [47]. We observed that the fluorophore remained fluorescent after its encapsulation into the SNPs and their attachment to the NT sidewalls. Therefore, the silica host was able to avoid fluorescence quenching caused by charge injection from metal-to-ligand charge-transfer excited states of the fluorophore into the conduction band of the NT quencher. This supramolecular fluorescent nanostructure, particularly one containing full-length pNTs, which have an intact π-electron structure, may be useful for a large variety of applications ranging from biosensors to electronics.

5. CONCLUSIONS

Carbon nanotube-nanoparticle assemblies are excellent building blocks for several applications ranging from electronic, biosensing, catalysis, and intracellular drug delivery. This chapter addresses the decoration of carbon nanotubes with metallic, semiconducting and insulating nanoparticles. The decoration with previously grown nanoparticles of both pristine and acid-oxidized nanotubes using either covalent or noncovalent chemistry was reported. Moreover, the in situ growth of nanoparticles onto nanotubes was described.

REFERENCES

1. M. S. Dresselhaus, G. Dresselhaus, and P. C. Eklund, *Physical Properties of Carbon Nanotubes*, London: Imperial College Press, (1998).
2. A. V. Ellis, K. Vijayamohanan, R. Goswami, N. Chakrapani, L. S. Ramanathan, P. M. Ajayan, and G. Ramanath, *Nano Lett.* 3, 279 (2003).
3. S. Fullam, D. Cottell, H. Rensmo, and D. Fitzmaurice, *Adv. Mater.* 12, 1430 (2000).
4. Y.-Y. Ou and M. H. Huang, *J. Phys. Chem. B* 110, 2031 (2006).
5. Z. Zhong, S. Patskovskyy, P. Bouvrette, J. H. T. Luong, and A. Gedanken, *J. Phys. Chem. B* 108, 4046 (2004).
6. L. Liu, T. Wang, J. Li, Z.-X. Guo, L. Dai, D. Zhang, and D. Zhu, *Chem. Phys. Lett.* 367, 747 (2003).
7. P. Corio, S. D. M. Brown, A. Marucci, M. A. Pimenta, K. Kneipp, G. Dresselhaus, and M. S. Dresselhaus, *Phys. Rev. B* 61, 13202 (2001).
8. K. S. Coleman, S. R. Bailey, S. Fogden, and M. L. H. Green, *J. Am. Chem. Soc.* 125, 8722 (2003).
9. K. Jiang, A. Eitan, L. S. Schadler, P. M. Ajayan, R. W. Siegel, N. Grobert, M. Mayne, M. Reyes-Reyes, H. Terrones, and M. Terrones, *Nano Lett.* 3, 275 (2003).
10. B. Kim and W. M. Sigmund, *Langmuir* 20, 8239 (2004).
11. J. Liu, A. G. Rinzler, H. Dai, J. H. Hafner, R. K. Bradley, P. J. Boul, A. Lu, et al., *Science* 280, 1253 (1998).
12. J. Hu, J. Shi, S. Li, Y. Qin, Z.-X. Guo, Y. Song, and D. Zhu, *Chem. Phys. Lett.* 401, 352 (2005).
13. B. M. Quinn, C. Dekker, and S. G. Lemay, *J. Am. Chem. Soc.* 127, 6146 (2005).
14. H. C. Choi, M. Shim, S. Bangsaruntip, and H. Dai, *J. Am. Chem. Soc.* 124, 9058 (2002).
15. L. Qu and L. Dai, *J. Am. Chem. Soc.* 127, 10806 (2005).
16. L. Brus, *Appl. Phys. A* 53, 465 (1991).
17. A. P. Alivisatos, *J. Phys. Chem.* 100, 13226 (1996).
18. S. Banerjee and S. S. Wong, *Nano Lett.* 2, 195 (2002).
19. J. M. Haremza, M. A. Hahn, and T. D. Krauss, *Nano Lett.* 2, 1253 (2002).
20. W. C. W. Chan and S. M. Nie, *Science* 281, 2016 (1998).
21. C. B. Murray, D. J. Norris, and M. G. Bawendi, *J. Am. Chem. Soc.* 115, 8706 (1993).
22. L. Qu, Z. A. Peng, and X. Peng, *Nano Lett.* 1, 333 (2001).
23. S. Ravidran, S. Chaudhary, B. Colburn, M. Ozkan, and C. S. Ozkan, *Nano Lett.* 3, 447 (2003).
24. M. Olek, T. Büsgen, M. Hilgendorff, and M. Giersig, *J. Phys. Chem. B* ASAP.
25. M. J. O'Connell, S. M. Bachilo, C. B. Huffman, V. C. Moore, M. S. Strano, E. H. Haroz, K. L. Rialon, et al. *Science* 297, 593 (2002).
26. S. Chaudhary, J. H. Kim, K. V. Singh, and M. Ozkan, *Nano Lett.* 4, 2415 (2004).
27. F. Balavoine, P. Schultz, C. Richard, V. Mallouh, T. W. Ebbesen, and C. Mioskowski, *Angew. Chem., Int. Ed.* 38, 1912 (1999).
28. J. S. Lenihan, V. G. Gavalas, J. Wang, R. Andrews, and L. G. J. Bachas, *J. Nanosci. Nanotechnol.* 4, 600 (2004).
29. N. W. S. Kam and H. Dai, *J. Am. Chem. Soc.* 127, 6021 (2005).
30. M. Bottini, F. Cerignoli, M. I. Dawson, A. Magrini, N. Rosato, and T. Mustelin, *Biomacromolecules* 7, 2259 (2006).
31. D. M. Guldi, G. M. A. Rahman, V. Sgobba, N. A. Kotov, D. Bonifazi, and M. Prato, *J. Am. Chem. Soc.* 128, 2315 (2006).
32. Q. Li, B. Sun, I. A. Kinloch, D. Zhi, H. Sirringhaus, and A. H. Windle, *Chem. Mater.* 18, 164 (2006).
33. S. Banerjee and S. S. Wong, *Chem. Commun.* 1866 (2004).
34. S. Banerjee and S. S. Wong, *J. Am. Chem. Soc.* 125, 10342 (2003).
35. H. Kim and W. Sigmund, *Appl. Phys. Lett.* 81, 2085 (2002).
36. H. Kim and W. Sigmund, *J. Cryst. Growth* 255, 114 (2003).
37. B. Liu and J. Y. Lee, *J. Phys. Chem. B* 109, 23783 (2005).
38. I. Robel, B. A. Bunker, and P. V. Kamat, *Adv. Mater.* 17, 2458 (2005).
39. C. Li, Y. Tang, K. Yao, F. Zhou, Q. Ma, H. Lin, M. Tao, and J. Liang, *Carbon* ASAP.
40. J. Du, L. Fu, Z. Liu, B. Han, Z. Li, Y. Liu, Z. Sun, and D. Zhu, *J. Phys. Chem. B* 109, 12772 (2005).
41. W.-Q. Han and A. Zettl, *Nano Lett.* 3, 681 (2003).
42. S. Lee and W. M. Sigmund, *Chem. Commun.* 780 (2003).
43. W. Stöber, A. Fink, and E. Bohn, *J. Colloid Interface Sci.* 26, 62 (1968).
44. R. P. Bagwe, C. Yang, L. R. Hilliard, and W. Tan, *Langmuir* 20, 8336 (2004).
45. M. Bottini, L. Tautz, H. Huynh, E. Monosov, N. Bottini, M. I. Dawson, S. Bellucci, and T. Mustelin, *Chem. Commun.* 758 (2005).
46. M. Bottini, A. Magrini, M. I. Dawson, A. Bergamaschi, and T. Mustelin, *Carbon* 44, 1298 (2006).
47. M. Bottini, A. Magrini, A. Di Venere, S. Bellucci, M. I. dawson, N. Rosato, A. Bergamaschi, and T. Mustelin, *J. Nanosci. Nanotechnol.* 6, 1381 (2006).